KSTLE International Journal, Vol. 3, No. 2, December 2002, pp. 84-89

Analysis of the Effects of Bore Clearance Due to Skirt Profile Changes on the Piston Secondary Movements

Siyoul Jang

School of Mechanical and Automotive Engineering, Kookmin University, 861-1, Chungnung-dong, Sungbuk-gu, Seoul, 136-702, Korea

Abstract : Clearance movements of engine piston are very related to the piston impact to the engine block as well as many tribological problems. Some of the major parameters that influence these kinds of performances are piston profiles, piston offsets and clearance magnitudes. In our study, computational investigation is performed about the piston movements in the clearance between piston and cylinder liner by changing the skirt profiles and piston offsets. Our results show that curved profile and more offset magnitude to thrust side have better performance that has low side impact during the engine cycle.

Keywords : Skirt profile, pin offset, piston slap impact, clearance design

Introduction

Clearance design is very important to many mechanical elements of moving parts in many aspects. Among the many moving mechanical components in the clearance, piston depends strongly on the skirt profile and the magnitude of clearance for the performance and endurance life. In general, tight clearance design makes many tribological problems with low noise and vibration, while loose clearance design have less friction and wear with higher side impact of piston to cylinder block. Because piston movement is under high pressure and sudden change of velocity, the clearance design of skirt profile influences the tribological problems and side impacts on the engine. Therefore, it is necessary to consider these both effects simultaneously for higher efficient engine that has low impact vibrations and tribological problems.

In order to investigate the movement of piston in the clearance between piston and cylinder block, verification of fluid film behaviors of hydrodynamic lubrication needs to be performed in advance. Many researches have been performed regarding this matter. However, most computations of hydrodynamic lubrication are studied with half Sommerfeld boundary condition [1,2] that does not consider the real hydrodynamic lubrication condition. In our work, the fluid film pressures are computed with three kinds of piston movements such as sliding, rolling and translation with Reynolds boundary condition during the engine cycle. Piston movements are traced in the clearance by equating the applied forces from combustion pressure and many other inertia forces with fluid film pressure.

†Corresponding author; Tel: 82-2-910-4831, Fax: 82-2-910-4836
E-mail: jangs@kookmin.ac.kr

Piston Skirt Profiles of Flat, Barell and 3 Pad Types

Better lubricant film of hydrodynamic lubrication exists when the sliding direction is to the narrower space of gap. Straight profile (flat type) can have lubrication film on the narrower gap of sliding direction (*i.e.* thrust side). However, piston have wider gap of sliding direction (*i.e.* anti-thrust side) on the other side, so the piston is not supported by the fluid film pressure and sometimes direct impact on the cylinder block occurs with large vibration, so called piston slap. When the skirt profile has curved feature of barrel type, it can have supports on both sides of piston skirts such as thrust and anti-thrust sides, so that the direct impact happens less frequently. Figure 1 shows the profile difference between straight and barrel shapes at 90 degree of piston pin assembly position (thrust and anti-thrust sides) and Fig. 2 shows surface shape of barrel type skirt.

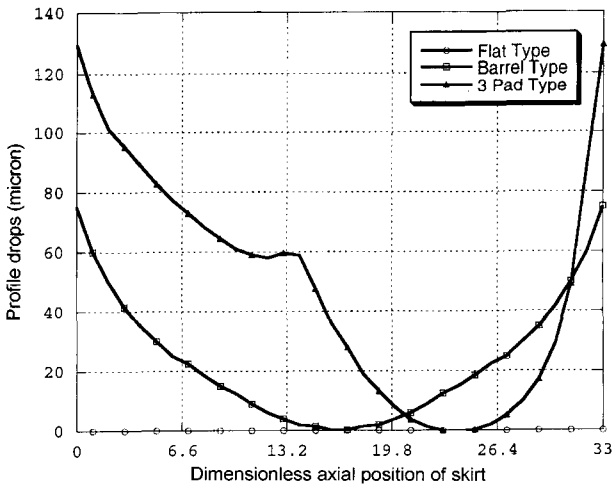

Fig. 1. Profiles of flat, barrel and 3 pad types of pistons.

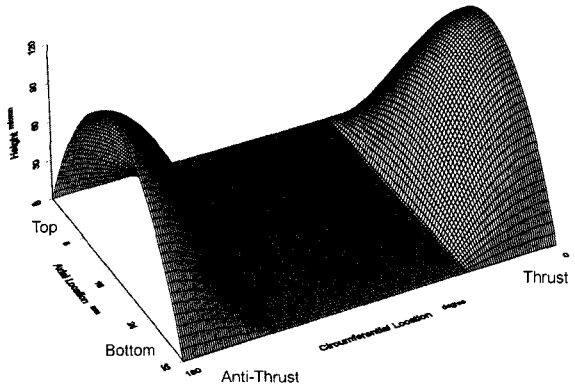

(a) Skirt shape of barrel type on thrust and anti-thrust sides

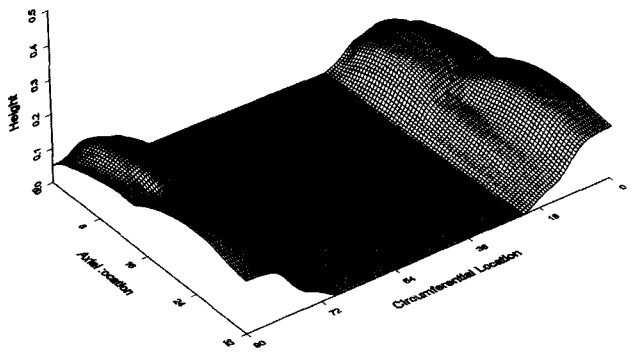

(b) Skirt shape of 3 pad type on thrust and anti-thrust sides

Fig. 2. Unwrapped skirt profiles of barrel and 3 pad type.

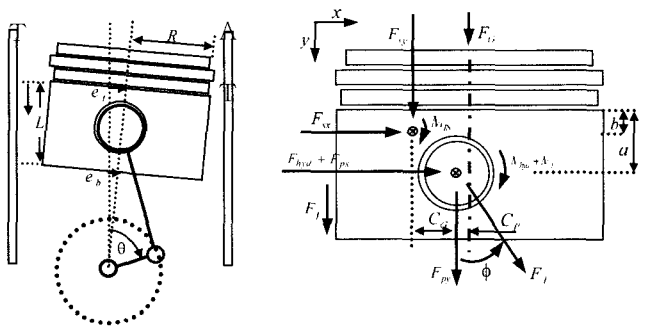

Fig. 3. Force and moment acting on piston.

Piston Movements in the Clearance

Piston slides in the bore clearance in the axial direction as well as translates in the lateral direction. If the clearance is large, the piston moves laterally with low friction but gives high impact on the cylinder block. Otherwise, it gives low impact but produces high frictional power loss and many tribological problems. In order to verify these effects, it is necessary to find out the forces acting on the piston components, such as piston skirt, piston pin, connecting rod, etc. Fig. 3 shows the forces on the piston components.

The foreces in the x and y directions are shown in Eq. 1 and 2 and moment about piston pin is shown in Eq. 3.

$$\sum F_y = F_G + F_f + F_{py} + F_{sy} + F_l\cos\phi = 0 \tag{1}$$

$$\sum F_x = F_{hyd} + F_{asp} + F_{px} + F_{sx} - F_l\sin\phi = 0 \tag{2}$$

$$\sum M_{pin} = M_{hyd} + M_f + M_{IS} + F_{sx}(a-b) - F_{sy}C_g + F_GC_p = 0 \tag{3}$$

With Eq.'s 1 and 2, the force equilibrium is obtained by deleting the force component along the connecting rod, F_l.

$$-F_{px} - F_{sx} = F_{hyd} + F_{asp} + F_f\tan\phi + F_{Wall} \tag{4}$$

Lateral Force F_{wall} is defined as in Eq. 5.

$$F_{Wall} = (F_G + F_{py} + F_{sy})\tan\phi \tag{5}$$

Similarly, the moment Eq. 4 is expressed as in Eq. 6

$$-M_{IS} - F_{sx}(a-b) = M_{hyd} + M_f + M_{Wall} \tag{6}$$

and the magnitude of moment due to lateral force, M_{wall} is shown in Eq. 7.

$$M_{Wall} = F_GC_p - F_{sy}C_g \tag{7}$$

Inertia forces and moment by piston and piston pin due to axial and lateral motions are described by the following Eq 8, 9 and 10.

$$F_{sx} = -m_{pis}\left(\ddot{e}_t - \frac{a}{L}(\ddot{e}_b - \ddot{e}_t)\right) \tag{8}$$

$$F_{px} = -m_{pin}\left(\ddot{e}_t - \frac{b}{L}(\ddot{e}_b - \ddot{e}_t)\right) \tag{9}$$

$$M_{IS} = \frac{I_{pis}(\ddot{e}_t - \ddot{e}_b)}{L} \tag{10}$$

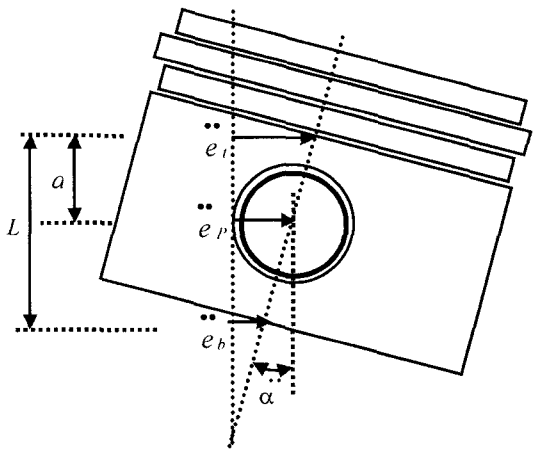

Fig. 4. Lateral inertia force acting on piston.

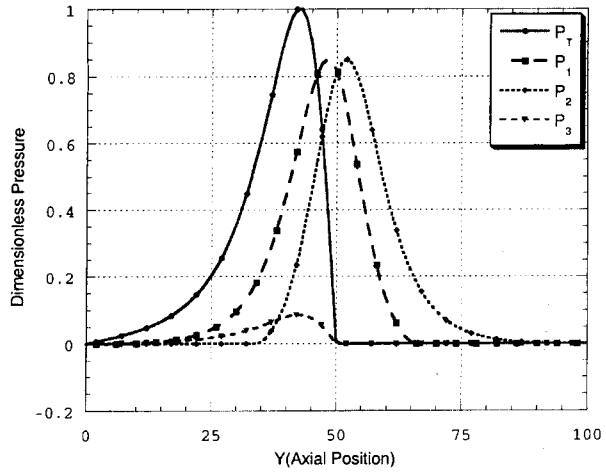

(a) Sommerfeld boundary condition for cavitation regime

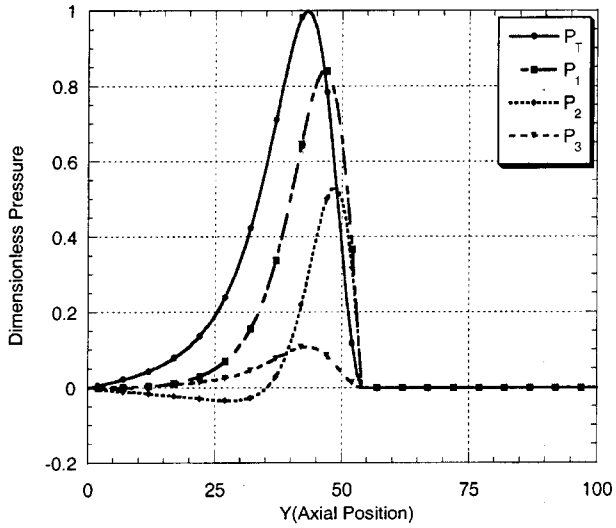

(b) Reynold's boundary condition for cavitation regime

Fig. 5. Pressure profile of each component of movement using Sommerefeld and Reynolds boundary condition and total pressure depending on the constants U^*, $d\varepsilon^*_b/dt$ and $d\varepsilon^*_t/dt$.

In order to find out the motions of piston in the bore clearance, system equation from the above Eqs. is expressed as in Eq. 11.

$$\begin{bmatrix} m_{pis}\left(1-\frac{b}{L}\right)+m_{pin}\left(1-\frac{a}{L}\right) & m_{pis}\frac{b}{L}+m_{pin}\frac{a}{L} \\ \frac{I_{pis}}{L}+m_{pis}(a-b)\left(1-\frac{b}{L}\right) & -\frac{I_{pis}}{L}+m_{pis}(a-b)\frac{b}{L} \end{bmatrix} \begin{bmatrix} \ddot{e}_t \\ \ddot{e}_b \end{bmatrix} = \begin{bmatrix} F_{hyd}+F_{asp}+F_f\tan\phi+F_{Wall} \\ M_{hyd}+F_{asp}+M_f+M_{Wall} \end{bmatrix} \tag{11}$$

Hydrodynamic Lubrication in the Bore Clearance

The force equilibrium between side force of piston and fluid film pressure is computed at each time step (720 steps) during

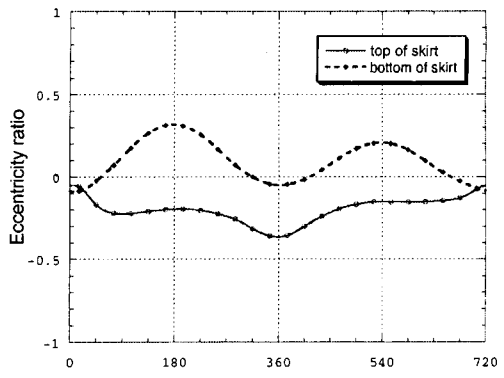

(a) c=20μm

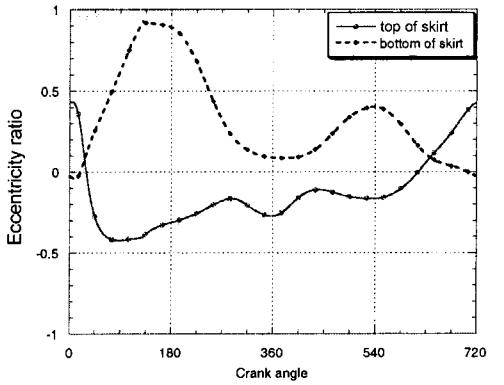

(b) c=40μm

Fig. 6. Piston movements according to the clearance sizes at 0.4 mm offset and 4000 rpm.

engine cycle by tracing the upper and lower positions of piston as it is done by Dursunkaya [1]. The forces on the piston come from combustion pressure, acceleration of piston components, fluid film pressures, (Eq. 12) by three kinds of movements such as translation, sliding and rotation. Many other researches have performed the computation of hydrodynamic lubrication pressure with half Sommerfeld boundary condition for three kinds of movements which have some physical simplications. In our study, we impose Reynolds boundary condition for the computation of fluid film pressure, which meets more physical conditions of piston movements as it is shown in Fig. 5. In the region of cavitation, none of the movements can make hydrodynamic lubrication pressures.

$$\frac{\partial}{\partial y^*}\left(h^{*3}\frac{\partial p^*}{\partial y^*}\right)+\frac{\partial}{\partial\theta}\left(h^{*3}\frac{\partial p^*}{\partial\theta}\right)= -U^*\left(\frac{(\varepsilon_b-\varepsilon_t)\cos\theta}{L^*}+\frac{\partial f(y^*,\theta)}{\partial y^*}\right)+\beta\left(\dot{\varepsilon}_t\cos\theta+(\dot{\varepsilon}_b-\dot{\varepsilon}_t)\frac{y^*}{L^*}\cos\theta\right) \tag{12}$$

Total pressure p^* is obtained by the summation of three kinds of movements as Eq. (2).

$$p^* = -U^*p_1^* + \dot{\varepsilon}_t p_2^* + (\dot{\varepsilon}_b-\dot{\varepsilon}_t)p_3^* \tag{13}$$

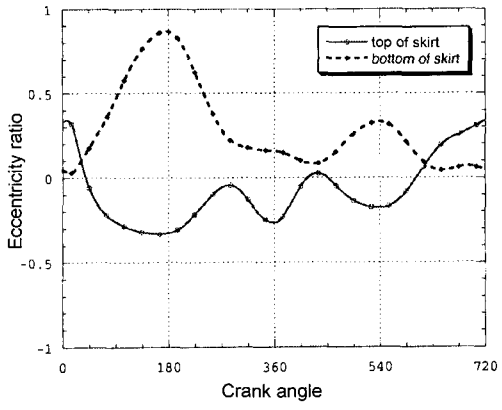

(a) flat type c=20μm

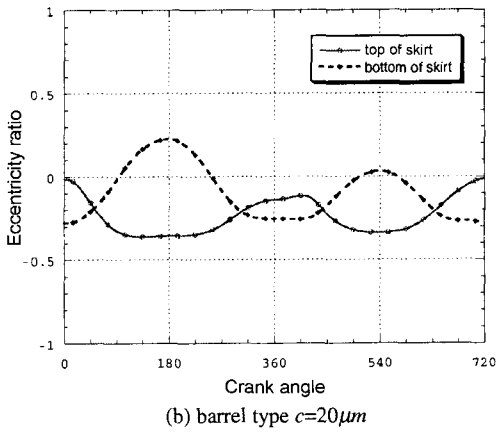

(b) barrel type c=20μm

Fig. 7. Piston movements according to skirt profiles at 0.4 mm offset and 4000 rpm.

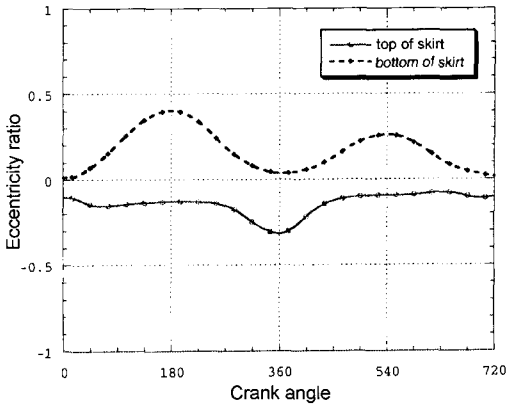

(a) offset =0.4mm

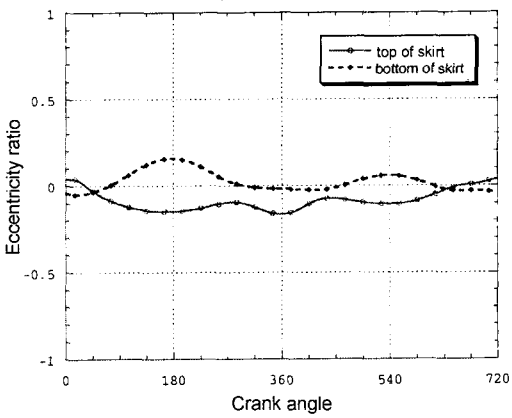

(b) offset=0.6mm

Fig. 8. Piston movements according to the clearance sizes at 0.4 mm offset and 4000 rpm.

for the pressure p_2* of sliding:

$$\frac{\partial}{\partial y^*}\left(h^{*3}\frac{\partial P^*}{\partial y^*}\right)+\frac{\partial}{\partial \theta}\left(h^{*3}\frac{(\partial P)^*}{\partial \theta}\right)= \left(\frac{(\varepsilon_b-\varepsilon_t)\cos\theta}{L^*}+\frac{\partial f(y^*,\theta)}{\partial y^*}\right) \tag{14}$$

for the pressure p_2* of translation:

$$\frac{\partial}{\partial y^*}\left(h^{*3}\frac{\partial P^*}{\partial y^*}\right)+\frac{\partial}{\partial \theta}\left(h^{*3}\frac{(\partial P)^*}{\partial \theta}\right)=\beta\cos\theta \tag{15}$$

for the pressure p_3* of rotation:

$$\frac{\partial}{\partial y^*}\left(h^{*3}\frac{\partial P^*}{\partial y^*}\right)+\frac{\partial}{\partial \theta}\left(h^{*3}\frac{(\partial P)^*}{\partial \theta}\right)=\frac{y^*}{L^*}\beta\cos\theta \tag{16}$$

Results

Regarding the effects of clearance size on the piston movements, it is found that large bore clearance can cause more side impact to the cylinder block as it is shown in Fig. 6. The upper and lower locations of piston agitate in wider range at $c = 60\ \mu m$ than at $c = 20\ \mu m$ as shown in Fig. 9 which simulates the piston movements with the same data of Fig. 6 (b).

Skirt profile of barrel type can have lower side impact than the flat type as shown in Fig. 7 at the same amount of clearance size, especially during the explosion period (0-180° crank angle degree).

In Fig. 8, it is shown that more piston pin offset to the thrust side (minus direction of eccentricity) makes very well aligning movement. This is also very useful design information for the piston assembly because it can reduce side impact (slapping) and noise and vibration.

The hydrodynamic pressures in the bore clearance are obtained in cases of flat and barrel types of piston skirts. Comparing the pressures in the thrust side between flat (Fig. 10) and barrel (Fig. 12) types, the pressure of barrel type has more spread pattern than flat type. From this computation result, the piston movement of barrel type has more mild translation in the direction of secondary motion. In the anti-thrust side, it shows that the hydrodynamic pressure of barrel type has higher load capacity in the lower region of skirt than the flat type piston. It means that the piston of barrel type has more possibility of lower vibration because the piston can be supported. On the other hand, the piston of flat type has the period of far less load capacity during explosion (Fig. 11). This means that the piston can give more high vibrational mode

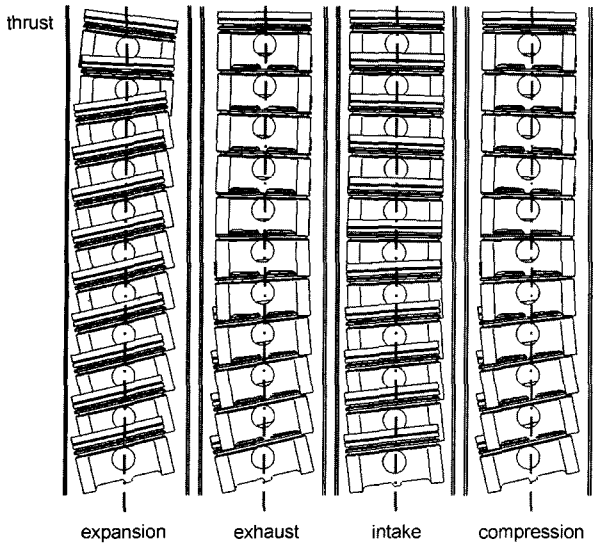

Fig. 9. Piston movements according to piston pin offset of 0.4 mm at 4000 rpm and c = 60 μm, (Fig. 6 (b)).

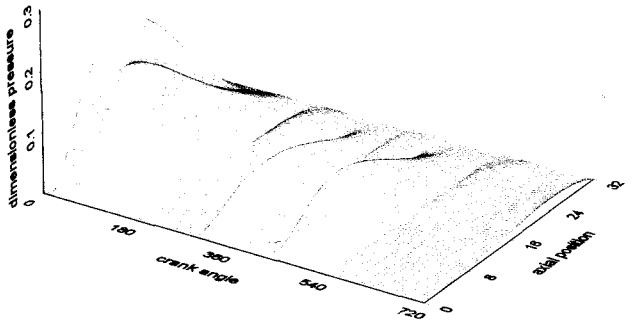

Fig. 10. Pressure distribution on the thrust side (flat type).

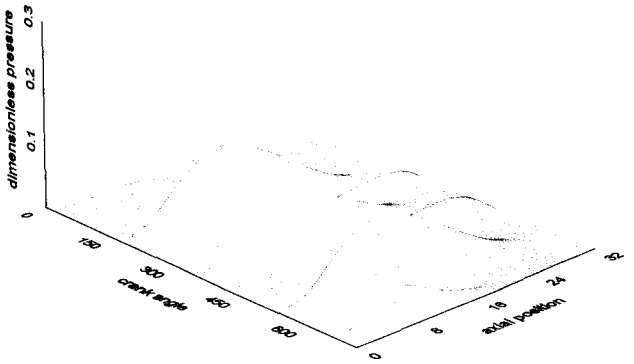

Fig. 11. Pressure distribution on the anti-thrust side (flat type).

than barrel type (Fig. 13).

Although three pad type of piston is design for low wear and friction, it provides more agitated pressure profiles on both thrust and anti-thrust sides. This is the reason that the computed hydrodynamic pressures around the pad are very sensitive to how the computational boundary and region are set.

The lower load capacity in flat type piston has more chances that thicker film thickness than in barrel type piston. Only

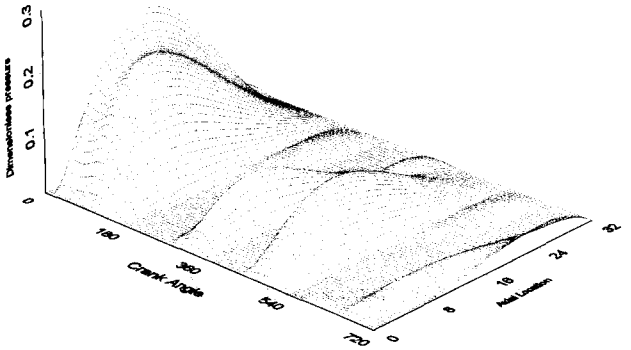

Fig. 12. Pressure distribution on the thrust side (barrel type).

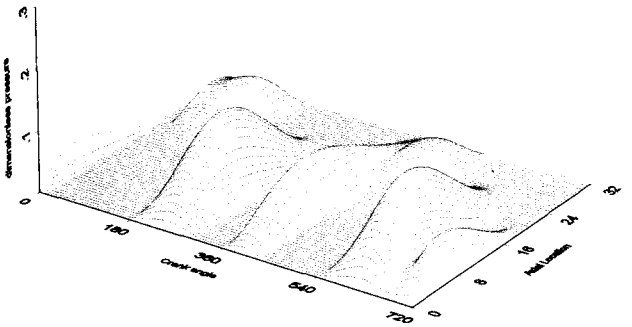

Fig. 13. Pressure distribution on the anti-thrust side (barrel type).

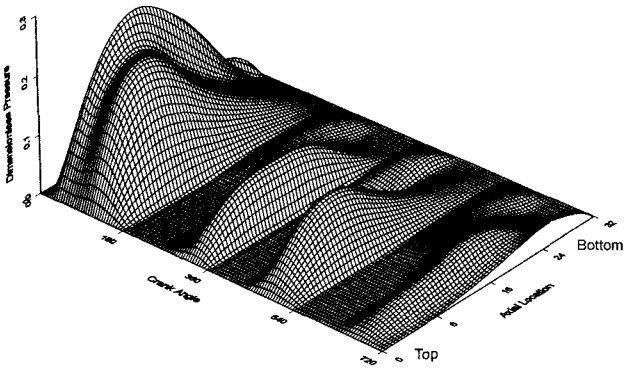

Fig. 14. Pressure distribution on the thrust side (3 pad type).

regarding the matter of viscous film thickness, flat type can have thicker film thickness because of low load capacity than barrel type. Therefore, flat type piston has higher film thickness than barrel type piston for the same applied load. Therefore, the viscous friction in case of flat type has higher value that in case of barrel type as shown in Fig. 16. As expected, the three pad type of piston has the smallest friction although it gives the most agitated load capcity.

Conclusion

In our work, we performed computational work of piston movement with the assumption of only hydrodynamic pressure in the clearance for the piston. For the design of less side impact to the cylinder liner, it is found that barrel type of skirt

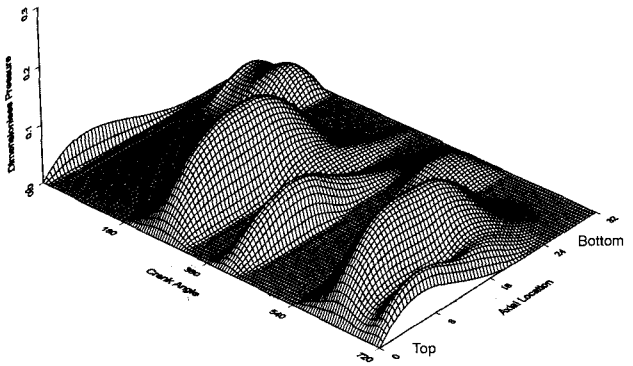

Fig. 15. Pressure distribution on the anti-thrust side (3 pad type).

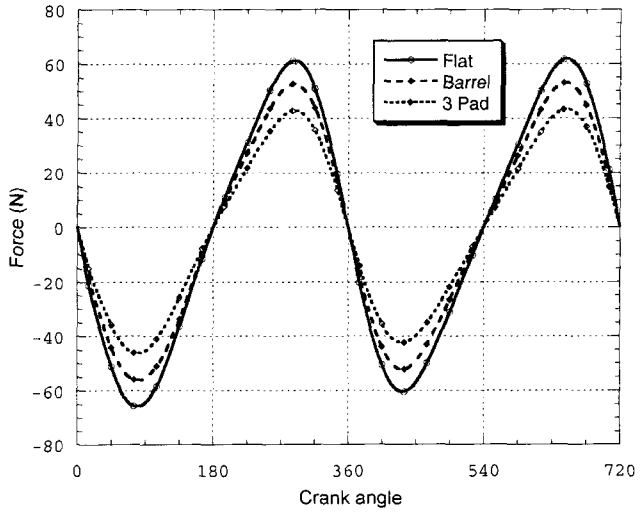

Fig. 16. Friction forces on the piston skirt by changing the profiles.

profile and small clearance and large piston offset can reduce side impact.

Acknowledgments

This work was supported by grant No. 2000-1-30400-005-3 from the Basic Research Program of the Korea Science & Engineering Foundation.

References

1. Zafer Dursunkaya and Rifat Keribar, "A Comprehensive Model of Piston Skirt Lubrication," SAE 920483, 1992.
2. Zafer Dursunkaya and Rifat Keribar, "Simulation of Secondary Dynamics of Articulated and Conventional Piston Assemblies," SAE 920484, 1992.
3. Kazuhide Ohta and Kiichi Yamamoto, "Piston Slap Induced Noise and Vibration of Internal Combustion Engines," SAE 870990, 1987.
4. Hamrock B.J, Fundamentals of Fluid Film Lubrication, McGraw-Hill, 1995.

Nomenclature

a :vertical distance from top of piston skirt to the piston center of mass. $[m]$
b :vertical distance from top of piston skirt to the wrist pin. $[m]$
c :radial clearance $[m]$
C_g :distance of the Piston center of mass from the wrist pin axis. $[m]$
C_p :wrist pin offset. $[m]$
e_t: eccentricity of piston at the top of skirt. $[m]$
e_b :eccentricity of piston at the bottom of skirt. $[m]$
F_{hyd} :load capacity of the hydrodynamic fluid film. $[N]$
F_G :combustion gas force. $[N]$
F_{sx} :lateral inertia force due to piston skirt mass. $[N]$
F_{sy} :axial inertia force due to piston skirt mass. $[N]$
F_{px} :lateral inertia force due to wrist pin mass. $[N]$
F_{py} :axial inertia force due to wrist pin mass. $[N]$
F_l :force along the connecting rod. $[N]$
F_f :viscous friction force. $[N]$
h :oil film thickness $[m]$
I_{pis} :moment of inertia of the piston about its center of mass. $[kg \cdot m^2]$
L :piston skirt length. $[m]$
l :connecting rod length. $[m]$
M_{hyd} :moment about wrist pin due to the hydrodynamic force. $[N \cdot m]$
M_f :moment due to viscous friction force. $[N \cdot m]$
M_{IS} :moment due to piston skirt inertia force. $[N \cdot m]$
M_{IP} :moment due to wrist pin inertia force. $[N \cdot m]$
m_{pis} :piston skirt mass. $[kg]$
m_{pin} :wrist pin mass. $[kg]$
P_{hyd} :hydrodynamic pressure. $[Pa]$
P_G :gas pressure. $[Pa]$
R :piston radius. $[m]$
r :crank arm length. $[m]$
t :time. $[s]$
U :piston axial velocity. $[m/s]$
X :lateral piston displacement. $[m]$
Y :axial piston displacement. $[m]$
y :fluid film axial coordinate measured from top of piston skirt. $[m]$
α :piston tilt angle $[rad]$
μ :lubricant viscosity. $[Pa \cdot s]$
ω :crankshaft rotational speed. $[s^{-1}]$

superscript*: dimensionless value